Construction and Building Materials 321 (2022) 125564

Contents lists available at ScienceDirect

Construction and Building Materials

journal homepage: www.elsevier.com/locate/conbuildmat

Mechanical and environmental characteristics of red mud geopolymers

Zengqing Sun [a], Qingyu Tang [a], Buhle Sinaye Xakalashe [b], Xiaohui Fan [a,*], Min Gan [a], Xuling Chen [a], Zhiyun Ji [a], Xiaoxian Huang [a], Bernd Friedrich [c]

[a] School of Minerals Processing and Bioengineering, Central South University, Changsha 410083, PR China
[b] Mintek, City of Johannesburg, South Africa
[c] Institute of Process Metallurgy and Metal Recycling, RWTH, Intzestr. 3, Aachen 52056, Germany

ARTICLE INFO

Keywords:
Red mud
Geopolymer
Environmental compatibility
Heavy metal
Trace element

ABSTRACT

Red mud is an industrial waste produced during the bauxite refining in the Bayer process. Increasing efforts have been recently paid to produce red mud geopolymers with feasible engineering properties. Meanwhile, the environmental compatibility of red mud geopolymers as construction material has not been clearly investigated. To facilitate clean production of red mud geopolymers, the release characteristics of Na, K, Al, Si, Ca, B, Ba, As, Cd, Co, Cr, Cu, Mn, Mo, Ni, Pb, Sb, Se, Sr, Tl, V, Zn, Cl^- and SO_4^{2-} from red mud geopolymers of different mixture proportions were investigated. Mechanisms dominating the release behaviors were also revealed. Results showed that red mud geopolymers significantly affect the chroma and turbidity of water body. Though the cumulative releases of most of the chemical components are in a similar range as cement-based materials, leaching of Pb, Sb and V in some cases surpass the environmental regulatory limits in Germany and the Netherlands. Preliminary analysis of release mechanism indicates that the leaching process is complex and mainly controlled by diffusion, while signs of surface wash-off, solubility and depletion are also detected.

1. Introduction

Red mud (RM) is the major waste of bauxite refining via Bayer process [1]. Bauxite, mainly composed of aluminium hydroxides, is the main source of aluminium production. During the Bayer process, bauxite is mixed with alkalis and exposed to conditions of elevated pressure and temperature [2,3]. Aluminium hydroxides in bauxite are extracted as sodium aluminate for following chemical processes, and RM is generated simultaneously [2]. As reported, approx. 150 million tons of RM are produced every year all over the world [4]. RM is high alkalinity (pH values around 10–12.5) and contains heavy metal and trace elements [5,6]. Disposal of RM not only requires huge areas of land but also possess serious environmental concerns.

Nowadays, increasing attention has been paid to the re-utilization of RM. Due to considerable amount of alumina is remaining in RM after the Bayer process, hydrometallurgy methods using sulfuric, citric and oxalic acids are developed [7]. Iron oxide is another typical major component of RM. Magnetic separation were applied for iron recovery as early as the 1970s [8–10]. The recovery efficiency could be significantly enhanced with high gradient superconducting magnetic separation system [11]. Pyrometallurgy in terms of roasting and reduction smelting processes, acid- and bio- leaching are also efficient methods for iron recovery [12–15]. Apart from recovering major components, practices are also made for the recovery of trace and rare earth elements. Depending on the quality of bauxite ore, the concentration of anatase or rutile titanium in RM ranges from 2.5% to 22.6% [6]. A titanium recovery of 64.5% was obtained by Agatzini-Leonardou et al. [16] using sulfuric acid leaching process. Ercag and Apak [17] developed a furnace smelting and extractive metallurgy to simultaneously recover titanium, iron and aluminium, and the titanium recovery efficiency was improved to 76%. Carbon adsorption and desorption route is normally used to extract vanadium from RM [18]. The Bayer process contributes to enrich scandium concentration in RM, with the general composition around 60–120 ppm [19,20]. Meanwhile, most scandium exists as associated minerals coupled with isomorphism [21,22]. Success has been made in selectively extracting scandium by acid leaching with the occurrence of tributyl phosphate modified activated carbon [23] or by combined ion exchange-solvent extraction method [20].

There are many other investigations aimed at utilizing RM as construction and building materials. Tsakiridis et al. [24] used RM as part of raw feedstocks for the production of cement clinkers. Results show that RM addition of 3.5% possessed no negative effects on the mineral

* Corresponding author.
E-mail address: csufanxiaohui@126.com (X. Fan).

https://doi.org/10.1016/j.conbuildmat.2021.125564
Received 31 August 2021; Received in revised form 16 October 2021; Accepted 3 November 2021
Available online 15 January 2022

composition and mechanical properties of obtained cement. Similar results were reported by Vangelatos et al. [25], Gordon et al. [26], Singh et al. [27] and Zhang et al. [28], respectively.

Geopolymer is a subset of alkali-activated material (AAM). First coined by French scientist Joseph Davidovits in the 1970s, geopolymer is now a robust alternative cementitious material [29,30]. The solid precursors most frequently used for geopolymer production include siliceous fly ash (FA) and metakaolin (MK), with the alkaline activators of sodium hydroxide, sodium silicate and their mixtures [31–34]. Studies have demonstrated that properties such as excellent mechanical strength, high-temperature resistance, strong adhesion to various surfaces, stability under chemical attacks, low cost, etc., can be obtained by well-produced geopolymer [27,33–35]. In addition, equivalent CO_2 emission of geopolymer was estimated up to 90% lower than cement counterpart.

Mixture of RM and FA was adopted by Zhang et al. [36] as solid precursor for geopolymer synthesis. The compressive strength of obtained geopolymer was not satisfactory, but improvement was made by the authors in [37]. Studies show that replacing FA by MK or ground granulated blast furnace slag (GGBS) contributes to improve the strength of RM geopolymer (RMG) [38,39]. Factors influencing reaction kinetics and strength evolution have been characterized in [40–43]. Efforts have also been paid in expanding the synthesis protocol. He et al. [44] produced RMG using rice husk ash as reactive precursor. In [45], one-part (just add water) RMG was developed via the alkali-thermal activation of RM. These practices contributed to optimise the production of RMG.

Meanwhile, all these practices focused on the synthesis procedure and the mechanical properties of obtained RMGs, with limited attention paid to the environmental compatibility of produced RMGs. Major components, heavy metals and trace elements might be released from RMGs into surrounding environment when getting contact with water. Studies focusing the stabilization property of geopolymer on artificially supplied components have been conducted [46–48]. However, these studies designed to evaluate the suitability of geopolymer for hazardous materials immobilization, and the matrixes are meant to be deposited. The release procesue, mechanism and limit are different with characterization framework for construction materials. To ensure that RMG-based construction materials meet environmental regulatory criteria, the release behaviours of chemical components should be evaluated before marketing. However, studies about this aspect have not been reported.

As part of environmental evaluation of RMG, this work is designed to reveal the release characteristics of Na, K, Al, Si, Ca, Cl^-, SO_4^{2-}, Ba, As, Cd, Co, Cr, Cu, Mo, Ni, Pb, Sb, Se, Sr, Tl, V, Zn from RMGs. A preliminary analysis of factors controlling the release process is also made. Comparison with release of cement-based materials, environmental regulatory limits in Germany and the Netherlands is included to provide a direct view of release characteristics of RMGs. All the results from this work contribute to raise the environmental concern about RMG and promote its environmentally compatible application.

2. Materials and methods

2.1. Materials

Two RMs, noted as RM-1 and RM-2, were used in this work. The chemical and mineral compositions of RMs, MK and GGBS were characterized using X-ray fluorescence (XRF) and X-ray diffraction, respectively. The bulk chemical composition is listed in Table 1, with the XRD results shown as Fig. S1 in supplementary. The MK is predominantly composed by SiO_2 and Al_2O_3. The SiO_2 and Al_2O_3 make up over 50 % of the GGBS in chemistry, with CaO accounting for 34.5 %. SiO_2, Al_2O_3 and CaO are reported as main reactive components during alkali activation. Different from MK and GGBS, significant amount of Fe_2O_3 is detected in both RMs. The total content of SiO_2, Al_2O_3 and CaO in RMs are less than in MK and GGBS.

All the solid precursors were digested in aqua regia solution for the determination of heavy metal and trace elements content. The measurement was conducted using Inductively coupled plasma mass spectrometry (ICP-MS). Results are listed in Table 2.

Sodium hydroxide and sodium silicates solutions are used as alkaline activators. The NaOH solution is 9 mol/l, which is prepared by dissolving analytical grade NaOH pellets in water. The sodium silicate solution originally contains 26.2 wt% SiO_2, 7.7 wt% Na_2O and 66.1 wt% H_2O (SiO_2/Na_2O molar ratio of 3.5). The SiO_2/Na_2O molar ratio was adjusted to 1.5 by adding sodium hydroxide pellets. Both activators were prepared and stored in airtight container for 24 h prior to use.

Five geopolymers were synthesized in this work, the mix proportions are shown in Table 2, which are determined based on laboratory pretests. For all mixtures, the sand to binder ratio was of 3.0. The sand used was CEN standard according to EN 196-1.

2.2. Sample preparation

Geopolymer mortars were produced in the following steps. The weighted solid precursors were firstly mixed in a planet mixer for 1 min, alkaline activator was then added and further mixed for 2 min. Standard

Table 2
Content of heavy metals and trace elements in GGBS, MK and RMs (given in mg/kg).

Parameter	GGBS	MK	RM-1	RM-2
Antimony	2.97	0.83	3.05	2.3
Arsenic	15.1	8.1	8.3	6.5
Barium	728	127	53	31
Lead	19.8	17.7	36.3	46.7
Boron	370	11	232	301
Cadmium	0.28	0.04	0.29	0.17
Chromium	35.7	72.6	45.4	52.1
Cobalt	13.3	2.9	9.8	4.6
Copper	35.4	5.6	19.1	31.2
Molybdenum	13.4	0.3	13.9	21.7
Nickel	36.0	36.5	24.6	18.9
Selenium	3.23	1.90	2.72	3.02
Strontium	838	36.6	49	63
Thallium	0.32	0.11	0.44	0.27
Vanadium	88.5	112.3	98.4	104.8
Zinc	46.3	29.9	46.0	40.3

Table 1
Chemical composition of MK, GGBS and RMs, given in % by weight.

	Al_2O_3	SiO_2	CaO	Fe_2O_3	MgO	TiO_2	Na_2O	K_2O	Chloride	Sulfur as SO_3
MK	32.6	61.2	0.1	1.2	0.2	1.6	0.2	0.6	0.01	0.07
GGBS	10.5	40.3	34.5	0.4	8.6	0.4	0.6	1.6	n.d.	2.19
RM-1	15.7	14.0	6.7	35.3	0.1	11.4	8.9	0.7	0.10	0.25
RM-2	23.0	5.5	10.2	44.0	0.1	5.6	1.8	0.9	0.08	0.17

n.d., none detected.

sand was filled into the mixer and mixed for another 3 min to get homogeneous mortar. Fresh mortar was then casted into 40 · 40 · 160 mm^3 moulds and vibrated 2 min. After being covered by glass plate, mortar together with moulds were transferred into curing box (20 °C and approx. 100 % relative humidity (RH)). Samples were demoulded after 24 h, sealed in plastic bags and transferred into curing room of 20 °C. Throughout sample preparation process, no thermal treatment was required (Table 3).

2.3. Strength measurement

The flexural and compressive strength were measured after 7d and 28 d curing, following DIN EN 196–1. For each geopolymer, three replicates were used for the flexural strength measurement. Three-point loading method was applied for the measurement with the distance between two supports being 100 mm. The load rate was 0.05 kN/s, which was applied at the mid span. The resultant six halves after flexural strength measurement were used for compressive strength measurement, for which the force rate was 2.4 kN/s.

2.4. Horizontal dynamic surface leaching

RMG mortars were cured for 28 days prior to the leaching test. Vessels with screw cap were used. Plastic bar spacers, 2 cm in thickness, were put in the vessels to ensure a distance between the sample and vessel. Sample surface areas were measured to determine water volume, i.e. the water volume is 80 l/m^2 of sample surface. Leachate was sampled and changed at 0.25, 1, 2.25, 4, 9, 16, 36, and 64 days. Blank tests, in which no geopolymer mortar was put, were also conducted. For every mix proportion, double-determination was applied, i.e., two mortar samples in each system were used for leaching.

After sampling, the pH value and electric conductivity of eluate were immediately measured. Na, K and Ca concentration was measured using flame photometry (ELEX 6361, Eppendorf), and Cl^- and SO_4^{2-} content was measured using ion chromatography (ICS 1100, DIONEX). The concentrations of Al, Si, As, B, Ba, Cd, Co, Cr, Cu, Mg, Mn, Mo, Ni, Pb, Sb, Se, Sr, Tl, V, Zn were then measured using ICP-OES (5110, Agilent) after acidifying the eluate with 5 vol% supra pure nitric acid.

After dividing individual measured concentration by the average concentration of all steps, the normalized concentration for each step was obtained (Eq. (1)). Based on the concentrations and eluate volume to sample surface ratio, cumulative release can then be calculated (Eq. (2)).

$$c_{N,i} = \frac{c_i}{\bar{c}} \tag{1}$$

$c_{N,i}$ normalized concentration of internal i

$\bar{c}$ the average concentration of the whole DSLT cycle, $\bar{c} = \frac{\sum_{i=1}^{8} c_i}{8}$.

$$E_n = \sum_{i=1}^{n} E_i = \sum_{i=1}^{n} (c_i - c_o)\frac{V}{O} \tag{2}$$

Table 3
Mix proportion of red mud geopolymer mortar, given in g.

	RM-1	RM-2	MK	GGBS	NaOH	Sodium Silicate	Sand
RMG-1	45	–	–	405	180	45	1350
RMG-2	225	–	–	225	180	45	1350
RMG-3	225	–	225	–	64	216	1350
RMG-4	–	225	–	225	180	45	1350
RMG-5	–	225	225	–	64	216	1350

E_n cumulative release at the end of interval n in mg/m^2
i sampling period, from 1 to 8
E_i release of interval i in mg/m^2
c_i concentration in the eluate in mg/l
c_0 background concentration in the blank in mg/l
V/O volume to surface ratio, V/O = 80 l/m^2.

3. Results and discussion

3.1. Flexural and compressive strength

Fig. 1 depicts the evolution of flexural and compressive strength of RMG mortars. Both the flexural and compressive strength are significantly influenced by binder formulation. It can be inferred by comparing RMG-1 with RMG-2 that increasing RM content results in the decrease of mechanical behaviour of obtained RMG. In addition, the influence of RM-1 and RM-2 on mechanical property of RMG is similar, reflecting as comparable flexural and compressive strength of RMG-2 with RMG-4, and RMG-3 with RMG-5. The MK-bearing geopolymers (RMG-3 and RMG-5) achieve better mechanical property than GGBS-bearing counterparts (RMG-2 and RMG-4) of similar RM content. This might be assigned to the higher reactivity of MK, which has been demonstrated in our previous studies [52,53]. Due to the higher fineness and layered structure of metakaolin, higher amount of liquid was required. Though the increased liquid-to-solid ratio possess some negative effect on pore structure, the corresponding activator content was also increased. This contributed to improve the geopolymerization, leading to the better mechanical property of RMG-3 and RMG-5.

Benefiting from the continuous reaction, both the flexural and compressive strength increase with the increase of curing time. And all the RMG mortars show good mechanical properties, with the 28 d compressive strength higher than 30 MPa. Moreover, three of the synthesized RMGs achieve 28 d compressive strength over 50 MPa. Though the RMG-2 exhibite the lowest mechanical property, the 28 d flexural and compressive strength are 8.9 MPa and 35.2 MPa. Both are better than many of the RMGs reported in [36–38,44,45,49]. The mechanical behaviours shown in Fig. 1 indicate that RMGs produced in this work are suitable for a broad civil engineering applications. Furthermore, no thermal pre-treatment such as alkali fusion is involved in this work and all the RMGs are produced at ambient condition, indicating that the RMGs synthesized in this work might be more environmentally friendly than reported in [36–38,44,45,49] and can be used for in-situ scenarios.

3.2. Eluate pH value, electric conductivity and chroma

Fig. 2 (a) depicts the pH values of eluates. The pH values are determined by several factors, such as the dosage of alkaline activator, physicochemical properties of solid precursors, reaction degree, etc. The sampling interval can also influence pH value since the leaching of chemical components is time related. Meanwhile the pH values of each system vary slightly throughout the whole DSLT, with the standard deviations (σ_{pH}) < 0.2. This might be assigned to the high alkalinity of

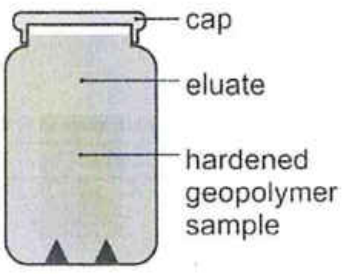

Fig. 1. Schematic representation of the leaching device.

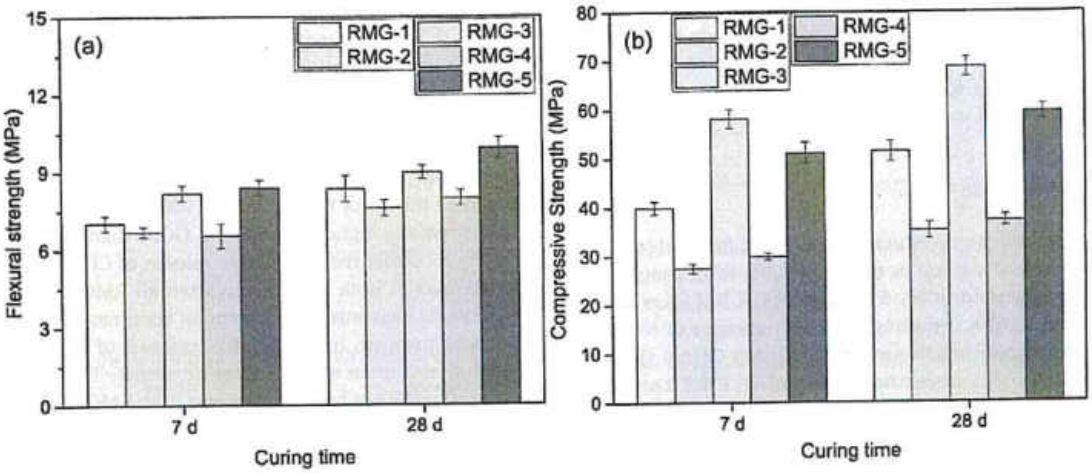

Fig. 2. Flexural (a) and compressive (b) strength of RMG mortars.

RMGs and no obviously change in solubility of mineral phases [50,52,55]. In comparison, GGBS-bearing RMGs (RMG-1, RMG-2 and RMG-4) exhibit higher pH values than the MK-bearing counterparts (RMG-3 and RMG-5). It should be mentioned that more activator was used for the synthesis of RMG-3 and RMG-5 than other RMGs. The higher rection degree might be responsible for the lower pH values of eluates.

The electrical conductivity of the eluates is shown in Fig. 2 (b). The RMG-1, RMG-2 and RMG-4 exhibit similar electricity patterns and the values are much higher than RMG-3 and RMG-5. As stated in [50,51], the electricity conductivity can be served as total ionic strength indicator. It can then be inferred that larger amounts of chemicals are leached from RMG-1, RMG-2 and RMG-4. Further discussions will be given in the following sections.

A qualitative analysis of eluate chroma and turbidity is taken into consideration in this work. As shown in Fig. 2 (c), the eluates of RMG-1 and RMG-2 look similar as the blank (deionized water), while the eluate of RMG-4 seems to be a little turbid. Colour of orange and light maroon can be clearly seen for the eluate from RMG-3 and RMG-5, respectively. The origin of the colour in eluate deserves further investigation. Though

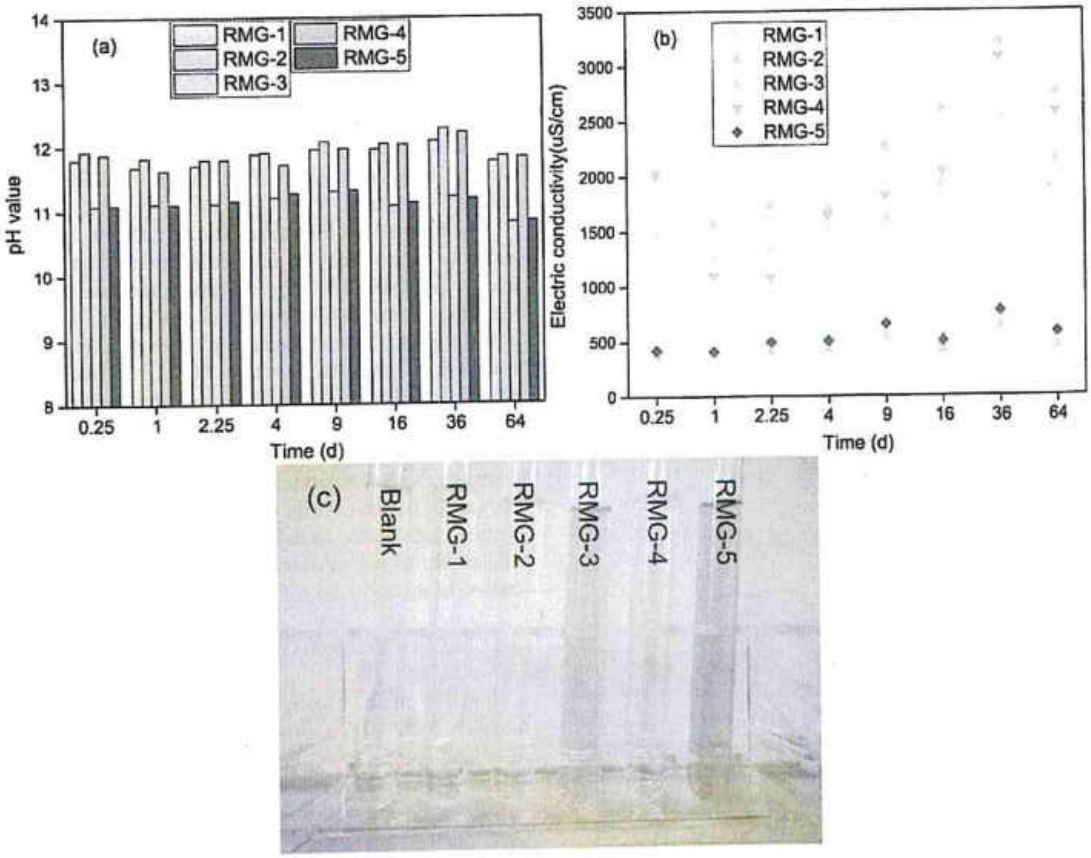

Fig. 3. The pH value, electric conductivity and photo of the eluates.

superior mechanical properties are achieved by RMG-3 and RMG-5, the obvious affection on chroma and turbidity of water body hinders their field application. Pre-treatment of RM-2 or optimization of synthesis procedure should be made to produce geopolymers that can be environmentally accepted used as construction material.

3.3. Leaching of major components

The predominant reaction product of RMG-3 and RMG-5 is the N-A-S-(H) gel, with Si and Al serving as the main framework components. Due to the high Ca content in GGBS, formation of C-A-S-H takes place in RMG-1, RMG-2 and RMG-4, resulting in the coexistence of N-A-S-(H) with C-A-S-H. The release behaviours of Si, Al and Ca are shown in Fig. 3. Higher amounts of Si are leached from RMG-1, RMG-2 and RMG-4 than from RMG-3 and RMG-5. It should be pointed out that the initial Si contents in RMG-3 and RMG-5 are higher than the others because of the high SiO_2 content of MK and larger adoption of sodium silicate activator. The low release results of Si from RMG-3 and RMG-5 might be ascribed to the reduced availability of Si in pore solution stemmed from the high reaction degree.

Compared with the release characteristics of Si, Al behaves on the contrary, i.e., higher amount of Al is leached from RMG-3 and RMG-5. A calculation of Al/Si ratio indicates that the eluate Al/Si ratios of RMG-3 and RMG-5 are higher than the corresponding ratio of the binders, while eluate Al/Si ratios lower than binders are found in RMG-1, RMG-2 and RMG-4. This means that Al is more easily leached than Si from RMG-3 and RMG-5, and vice versa. Preferential release or incongruent dissolution of geopolymers have been reported in [52,53]. This can be related to the partitioning property of Si and Al in reaction products and pore solutions, as well as the stoichiometry of gels. Further investigations are required to deepen understanding about the chemistry and stability of geopolymers.

In terms of the cumulative release, the release of Ca can be classified into three groups. The largest amount of Ca was released from RMG-1. RMG-2 and RMG-4 showed comparable Ca release, which is lower than RMG-1 but higher than RMG-3 and RMG-5. This follows the initial Ca content in the binders. The proportion of GGBS in RMG-1 is higher than in RMG-2 and RMG-4, contributing to the highest initial Ca content. Though the same mixing ratio is applied for RMG-2 and RMG-4, the RM-2 is composed of more CaO than RM-1, resulting in higher Ca content of RMG-4 than RMG-2. The same explanation can be applied for the release results of RMG-3 and RMG-5.

The release characteristics of Na and K from RMG mortars are shown in Fig. 4. The extremely high release of Na from all systems is assigned to

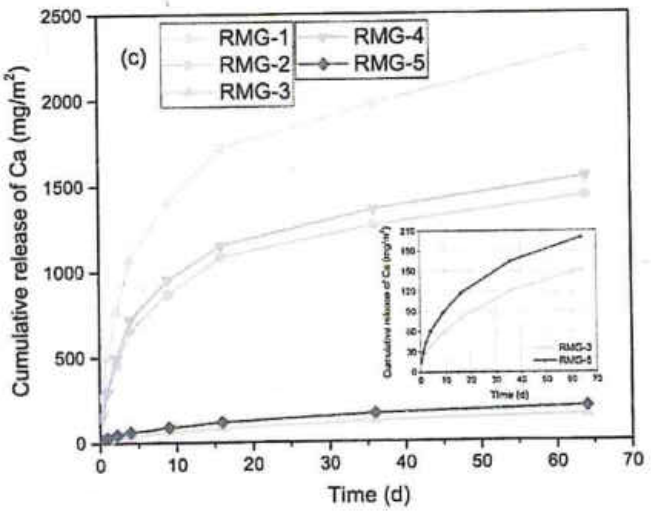

Fig. 4. Cumulative release of Si (a), Al (b) and Ca (c) from RMG mortars.

the adoption of sodium-based activators. In comparison, higher amount of Na is leached from RMG-1, RMG-2 and RMG-4 than the others. Similar phenomenon is observed for the release of K. In spite of that RMG-3 and RMG-5 are composed of higher initial Na content, the higher release of Na from RMG-1, RMG-2 and RMG-4 might be caused by slight lower reaction degree, leaving unreacted alkali mobile in pore solutions. In contrast, the K is originated from solid precursors. The higher cumulative release of K from RMG-1, RMG-2 and RMG-4 can be attributed to the initially higher K content in GGBS than in MK.

Fig. 5 shows the cumulative release of Cl^- and SO_4^{2-}. The release behaviours of both components from all RMG are similar. The above-mentioned elements show a trend of continuous increase of cumulative release, however, the cumulative releases of Cl^- and SO_4^{2-} gradually reach a maximum after 16 days of release. This reflects the gradually reduced release of both components from RMGs into eluate, indicating a depletion of leachable part. In [52,53], both Cl^- and SO_4^{2-} have been demonstrated as readily soluble species in geopolymers and the release is controlled by availability.

3.4. Leaching of heavy metal and trace elements

The leaching of heavy metal and trace elements from geopolymers into water is important for the environmental characterization. In this work, the release of B, Ba, As, Cd, Co, Cr, Cu, Mn, Mo, Ni, Pb, Sb, Se, Sr, Tl, V and Zn were considered. The cumulative releases of these components are calculated and listed in Table 4. It can be inferred that the releases of heavy metal and trace elements are influenced by the initial content, binder formulation, reaction degree, chemical state, etc. The release results of 167 cement-based materials derived from [54–56] are given in Table 4.

Compared with the cement-based materials and the limits in Germany and the Netherlands, the releases of most of the studied components are in a similar range as cement-based materials and meets the thresholds. Meanwhile, the cumulative releases of Pb from RMG-1, RMG-2, RMG-4 and RMG-5 surpass the German threshold, the release of Sb from RMG-3 and RMG-5 is higher than the German and Dutch imit values (Sb from RMG-4 is also over the German threshold). Though the German limit value on V is currently suspended, the releases of V from all RMGs exceed it.

Fig. 6 shows the release results of Cr, Cd, Zn, Pb, V and Mo from RMG mortars. High release of these components from RMG mortars at early ages is achieved, reflecting as repaid increase of cumulative releases. With the extension of release time, the cumulative release of Cr, Cd, Pb and Zn gradually approaches or closes to a maximum. Meanwhile, a calculation shows that less than 30% of Cd and 10% of Cr, Pb and Zn were leached from RMGs. This indicates the reduced release of these elements influenced by low leachable content [53]. The partitioning of these components in RMG deserves in-deepth characterization. In contrast, trend of continuous increase of the cumulative release of V and Mo can be seen from Fig. 6 (e) and (f). Apart from the high initial contents of both elements in RMG binders, the high mobility of V and Mo might also be responsible. The corresponding mechanisms will be discussed in section 3.5.

3.5. Leaching mechanism of studied components

Beyond characterizing the release characteristics of chemical components from RMG mortars, this work also investigates the primary leaching mechanisms. Potential factors controlling the leaching of chemical components from monolithic matrixes include surface wash-off, diffusion, solubility and/or depletion [54,58]. Methods have been developed to analyse the leaching mechanism. In CEN/TS 16637-2, a three-step diagram analysis protocol is suggested, in which key values of normalized concentrations (0.5, 1.0, 2.0) are provided. A three-step-diagram (such as Fig. 7 (a)) indicates diffusion-controlled leaching process. While, solubility-controlled leaching is reflected as normalized

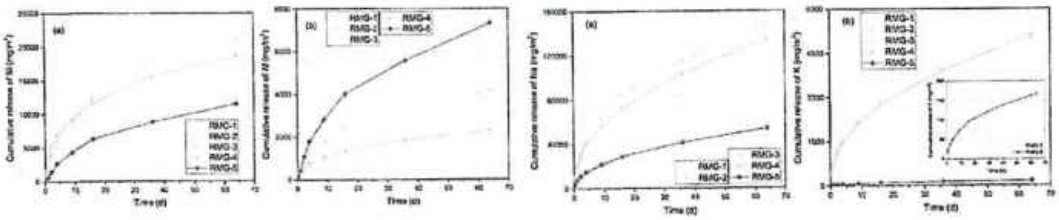

Fig. 5. Cumulative release of Na (a) and K (b) from RMG mortars.

Table 4
Cumulative release of heavy metal and trace elements from RMG mortars, in mg/m^2.

Element	RMG-1	RMG-2	RMG-3	RMG-4	RMG-5	CEM [a]	German Threshold [c]	Dutch Threshold [d]
As	3.21	2.60	3.15	4.07	4.26	0.017–11	11	260
Se	3.81	3.64	2.43	4.01	3.92	0.1–4.3	7.69	4.8
B	148.24	106.67	54.4	117.97	86.62	0.28–8.6	813	*
Cr	0.86	0.97	0.74	1.00	0.90	0.18–34	7.7	120
Cu	0.97	1.09	2.31	0.95	2.56	0.021–22	15.4	98
Mo	22.82	25.88	21.01	27.82	21.18	0.069–3.5	38.6	144
Mn	1.45	1.46	0.96	1.37	1.48	–	*	*
Pb	8.47	8.5	6.48	11.94	10.52	0.006–28	7.7	400
Tl	0.34	0.4	0.25	0.27	0.13	0.004–0.66	0.88	*
V	20.88	39.97	137.43	56.41	173.39	0.037–61	4.4[e]	320
Ba	83.16	7.51	4.96	49.05	1.09	0.59–496	375	1500
Cd	0.36	0.31	0.23	0.29	0.17	0.001–0.51	0.56	3.8
Co	2.56	1.96	4.34	1.92	3.05	0.036–3	8.8	*
Ni	1.49	2.05	3.26	1.69	3.84	0.16–23	15.4	81
Sb	1.45	1.01	0.63	0.49	0.33	0.007–5.4	5.5	8.7
Sr	25.13	11.45	0.16	18.22	0.12	–	*	*
Zn	5.17	9.33	6.08	7.98	9.94	0.12–67	63.9	800

[a] leaching results of cement based materials, data from [54], [55] and [56].
[b] average of release results of cement based materials, data from [55] and [56].
[c] German threshold [57].
[d] threshold in the Netherlands [56].
[e] the threshold is currently suspended.
* no threshold at the time being.

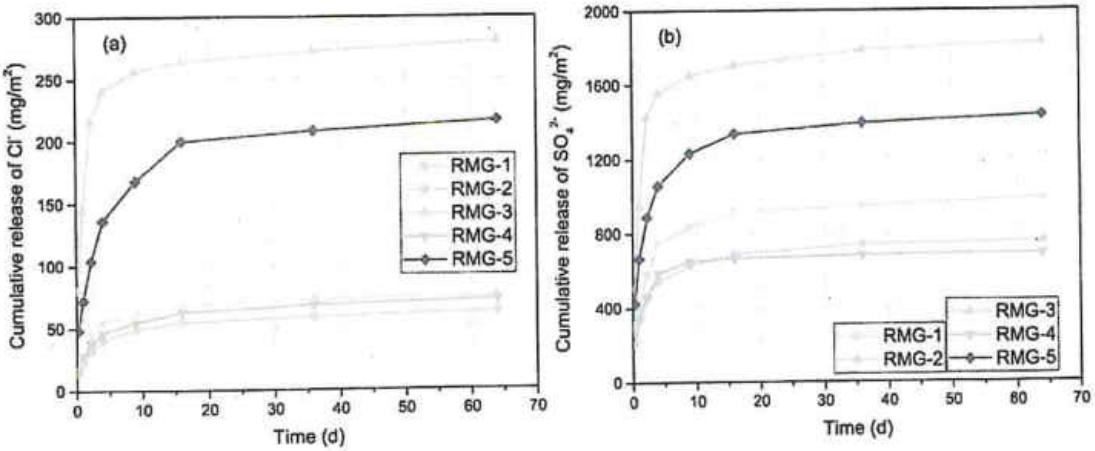

Fig. 6. Cumulative release of Cl (a) and SO_4^{2-} (b) from RMG mortars.

concentration appro. 1 at all leaching steps. Detailed description about the analysis procedure of leaching mechanism is referred to [53,59].

The normalized concentrations of Na, Ca, Si and Al are exemplarily shown in Fig. 7. As can been seen that the normalized concentrations of Na, Si and Al from all RMG mortars as well as the normalized concentrations of Ca from RMG-3 and RMG-5 roughly satisfies the three-step-diagram characteristics, thus the leaching process can be classified as diffusion controlled. By contrast, the normalized concentrations of Ca from RMG-1, RMG-2 and RMG-4 are around 1, meeting the solubility controlled leaching characteristics. The difference in leaching characteristics of Ca indicates its divergent chemical states in RMGs. During the reaction of RMG-1, RMG-2 and RMG-4, significant precipitation of Ca as C-A-S-H was detected. Meanwhile, RMG-3 and RMG-5 are of Ca-poor characteristic, dissolved calcium ions during reaction are in pore solution or modify the N-A-S(H) gel as (N, C)-A-S-(H) [60,61]. The differences in chemistry might possess influence on the leaching behaviours.

Though the leaching of Si and Al can be considered as diffusion controlled. The normalized concentrations of both components from RMG-3 and RMG-5 at early ages are much lower than target values. This

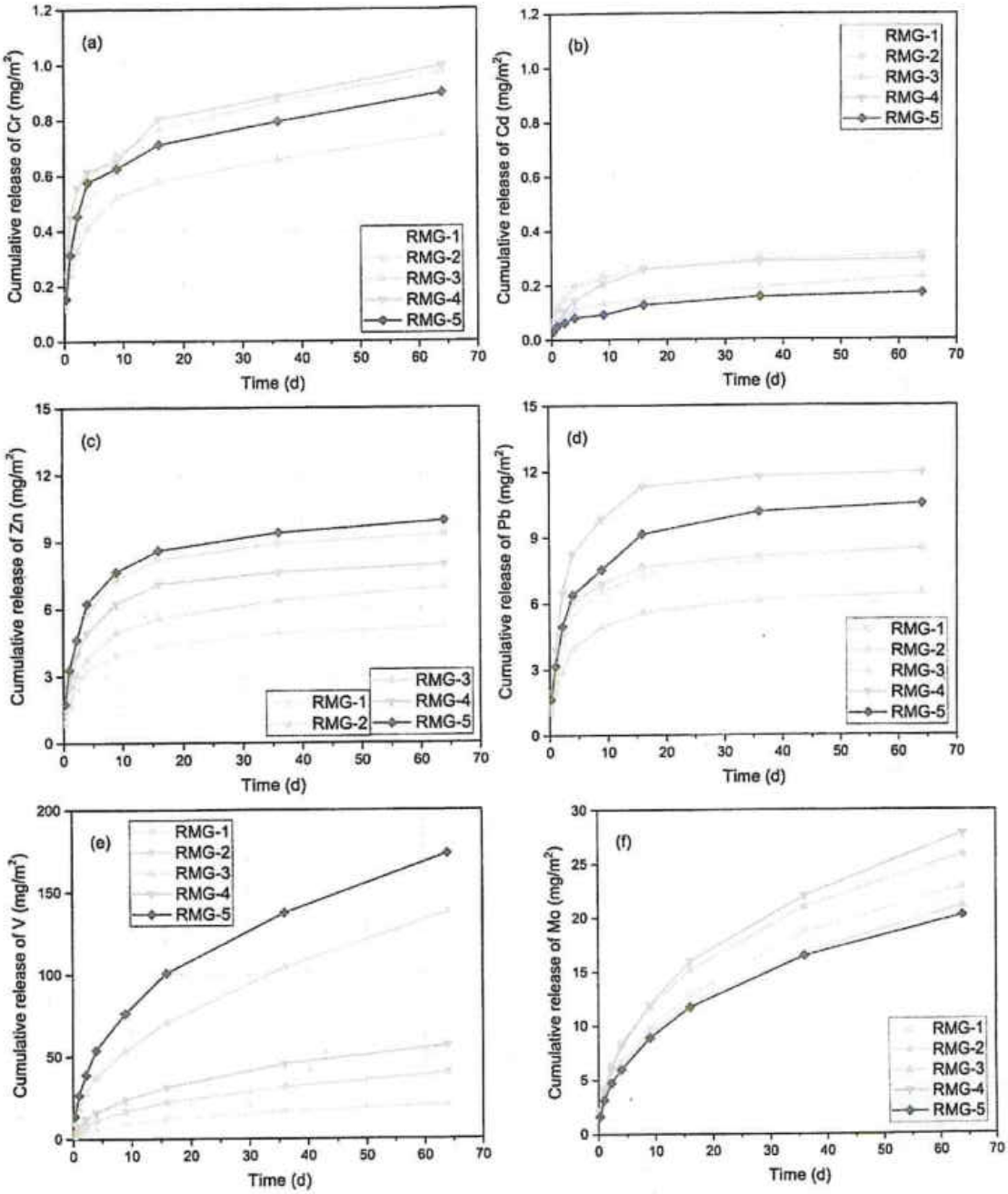

Fig. 7. Cumulative release of Cr (a), Cd (b), Zn (c), Pb (d), V (e) and Mo (f) from RMG mortars.

phenomenon can be regarded as delayed release. As stated by van der Sloot [55], there might be solubility controlling phases on sample surface that limit the leaching of the elements. Advanced characterization of samples coupled with geochemical modelling are ongoing to reveal the related mineralogical phases. In addition, surface-wash is involved in above release scenarios, reflecting as slightly higher normalized concentration at the beginning of leaching test.

The normalized concentrations of Cr, Cd, Pb, Zn, V and Mo are shown in Fig. 8. It should be mentioned that the mechanism analysis herein is limited to the leachable part of these components. For Cr and Cd, the normalized concentrations vary throughout the whole leaching process. This can be caused by the low available content of both elements in RMG binders. The c_{2-8} (average concentration of eluates 2–8) divided by the detection limit is smaller than 1.5, which confirms the leaching characteristics of inadequate leachable content. Though not shown here, the leaching of Sr from RMGs shows a similar trend.Fig. 9.

As shown in Fig. 8 (c) and (d), the normalized concentrations of Pb and Zn meet neither solubility nor diffusion controlled leaching pattern, but gradually decrease of normalized concentration can be seen. Further comparing c_7 and c_8 shows that $\frac{c_8}{c_7} < 0.9$, demonstrating that depletion of the small leachable fraction is involved in the leaching of both components from RMG mortars. Leaching of Cu, Ni and Mn from RMG is similar. Meanwhile, diffusion or solubility can not be fully excluded from the leaching process. Depending on the initial content and the physicochemical properties, these heavy metals can form precipitates of low solubility or participate in pore solution [47,62–65]. Detailed characterization of the chemical states is required to better reveal the leaching mechanism.

The release of V and Mo can be characterized as diffusion-controlled leaching, with the normalized concentrations satisfying the three-step-

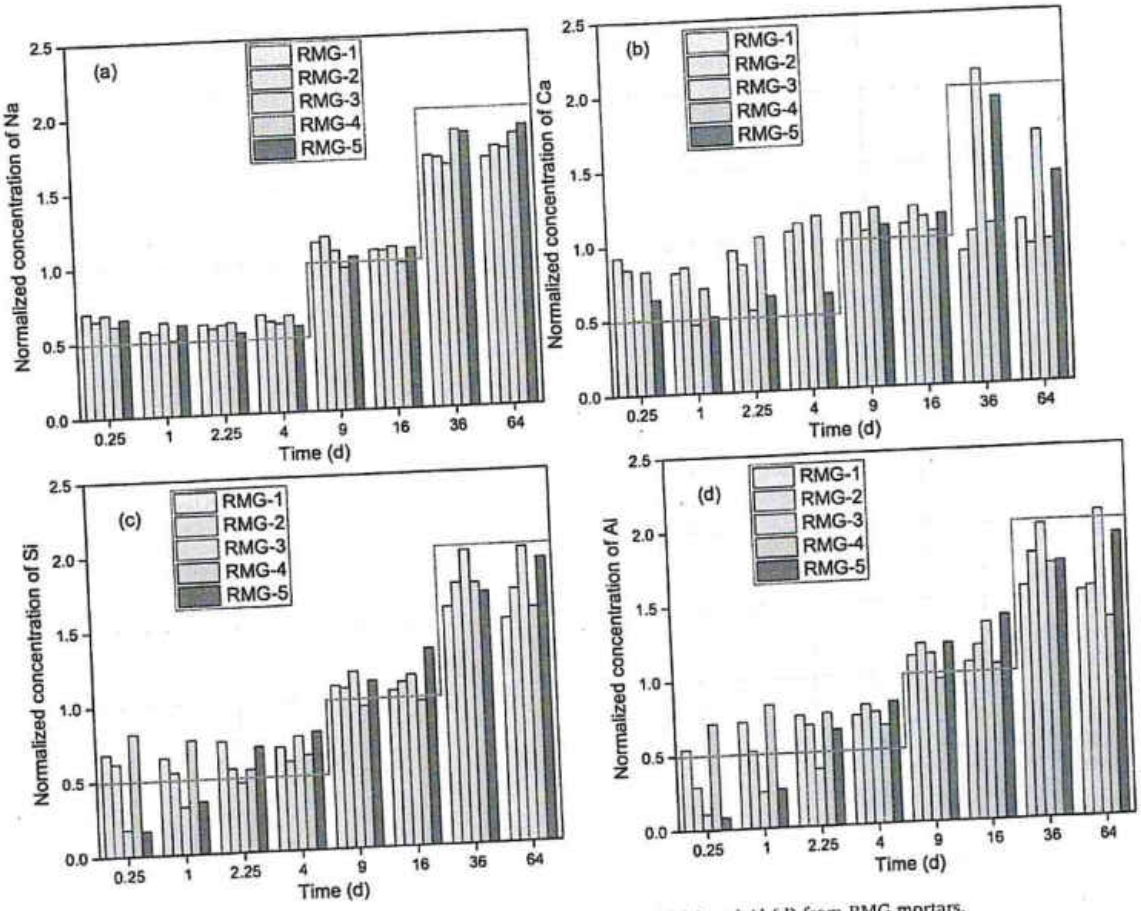

Fig. 8. Normalized concentration of Na (a), Ca (b), Si (c) and Al (d) from RMG mortars.

diagram characteristic (Fig. 8 (e) and (f)). Analogue transition was also observed for B and Se. Similar leaching characteristic was also found in the release of fly ash geopolymer and metakaolin geopolymer [53]. As listed in Table 4, the cumulative releases of B, Se, Mo and V are higher than other components. Apart from the high initial content, the high mobility of these elements might also matter. It has been demonstrated in [52] that these elements are mainly present as oxyanions. Like the transformation of V into VO_4^{3-}, element closing to oxygen in electronegativity tends to form oxyanion with the chemical bonding between oxygen and metal being covalent [52]. High mobility of these components was detected in the most acidic condition (pH < 2) as well as pH 9–12 [52]. As shown in Fig. 2, the pH values of eluates are around 11–12, favouring the high leaching of these components from RMG mortars. The special partitioning characteristics, as well as the low 64 d cumulative release and high normalized concentration suggest that the leaching of V and Mo can continue until deplection.

4. Summary and conclusion

The mechanical strength and leaching of chemical components from RMG was characterized in this work. Following conclusions can be drawn:

(1) The 28 d compressive strength of RMG ranged from 35.2 MPa to 68.7 MPa, which significantly depended on binder formulation. Increasing RM content resulted in the decrease of mechanical behaviour of obtained RMG, and MK-bearing RMGs possessed better mechanical property than GGBS-bearing counterparts.

(2) The pH values remained around 11–12 with slight fluctuation throughout the whole test. RMGs containing GGBS showed higher pH values than MK-bearing RMGs, while the latter obviously affect the chroma and turbidity of water body.

(3) In terms of the leaching of major components, larger amounts of Si, Ca, Na and K were leached from GGBS-bearing RMGs, while the leaching of Al, Cl^- and SO_4^{2-} behaved on the contrary.

(4) The cumulative releases of most of the studied heavy metal and trace elements were comparable with cementitious materials and met the thresholds. Meanwhile, the cumulative releases of Pb, Sb and V in some cases were higher than cement counterparts and surpassed the limit values.

(5) Leaching mechanism analysis showed that diffusion was the predominant controlling factor for the release of major components, heavy metal and trace elements. Signs of surface wash-off, solubility and depletion were also detected.

Apart from the above findings, attention would be made to further reveal the chemical states of above components within geopolymer. Influence of pore structure and pore solution on the release will be investigated. Cross-checking with other state-of-the-art techniques is planned to optimise the preparation and promote the environmentally compatible application of RMGs.

CRediT authorship contribution statement

Zengqing Sun: Writing – original draft. **Qingyu Tang:** Investigation, Validation. **Buhle Sinaye Xakalashe:** Resources, Validation. **Xiaohui Fan:** Supervision. **Min Gan:** Writing – review & editing. **Xuling Chen:** Project administration, Data curation. **Zhiyun Ji:** Data curation, Visualization. **Xiaoxian Huang:** Data curation, Visualization. **Bernd Friedrich:** Resources, Validation.

Declaration of Competing Interest

The authors declare that they have no known competing financial

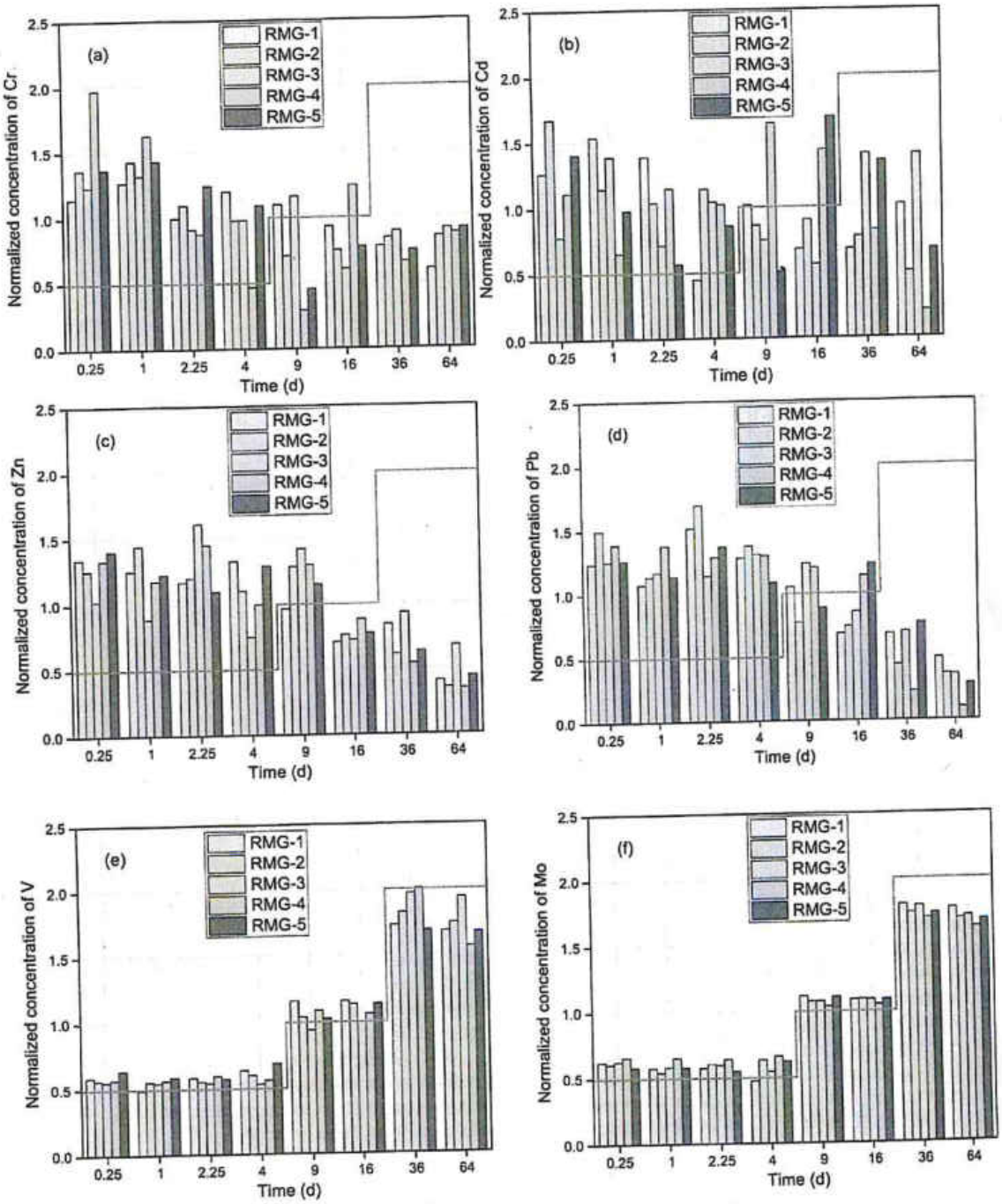

Fig. 9. normalized concentrations of Cr (a), Cd (b), Pb (c), Zn (d), V (e) and Mo (f).

interests or personal relationships that could have appeared to influence the work reported in this paper.

Appendix A. Supplementary data

Supplementary data to this article can be found online at https://doi.org/10.1016/j.conbuildmat.2021.125564.

References

[1] R.K. Paramguru, P.C. Rath, V.N. Misra, Trends in red mud utilization-a review, Miner. Process. Extr. M. 26 (2004) 1–29.
[2] A.T. Tabereaux, R.D. Peterson, Chapter 2.5 – Aluminum production, in: S. Seetharaman (Ed.), Treatise on Process Metallurgy, Elsevier, Boston, 2014, pp. 839–917.
[3] K.H.J. Buschow, R.W. Cahn, M.C. Flemings, B. Ilschner, E.J. Kramer, S. Mahajan, P. Veyssière, Encyclopedia of Materials, Science and Technology, Elsevier Ltd., 2001.
[4] S. Vigneshwaran, M. Uthayakumar, V. Arumugaprabu, Potential use of industrial waste-red mud in developing hybrid composites: A waste management approach, J. Clean. Prod. 276 (2020) 124278.
[5] Y. Liu, C. Lin, Y. Wu, Characterization of red mud derived from a combined Bayer Process and bauxite calcination method, J. Hazard. Mater. 146 (2007) 255–261.
[6] M. Gräfe, G. Power, C. Klauber, Bauxite residue issues: III. Alkalinity and associated chemistry, Hydrometallurgy 108 (1-2) (2011) 60–79.
[7] Z. Liu, H. Li, Metallurgical process for valuable elements recovery from red mud-a review, Hydrometallurgy 155 (2015) 29–43.
[8] S. Agrawal, V. Rayapudi, N. Dhawan, Extraction of iron values from red mud, Mater. Today Proc. 5 (9) (2018) 17064–17072.
[9] Y. Yang, X. Wang, M. Wang, H. Wang, P. Xian, Recovery of iron from red mud by selective leach with oxalic acid, Hydrometallurgy 157 (2015) 239–245.

[10] W. Liu, J. Yang, B.o. Xiao, Application of Bayer red mud for iron recovery and building material production from alumosilicate residues, J. Hazard. Mater. 161 (1) (2009) 474–478.
[11] T. Ohara, H. Kumakura, H. Wada, Magnetic separation using superconducting magnets, Physica C 357 (2001) 1272–1280.
[12] T.C. Eisele, K.L. Gabby, Review of reductive leaching of iron by anaerobic bacteria, Miner. Process. Extr. M. 35 (2014) 75–105.
[13] D. Uzun, M. Gulfen, Dissolution kinetics of iron and aluminium from red mud in sulphuric acid solution, Indian J. Chem. Techn. 14 (2007) 263–268.
[14] D.Q. Zhu, T.J. Chun, J. Pan, Z. He, Recovery of Iron From High-Iron Red Mud by Reduction Roasting With Adding Sodium Salt, J. Iron Steel Res. Int. 19 (2012) 1–5.
[15] R. Kumar, J. Srivastava, Premchand, Utilization of iron values of red mud for metallurgical applications, 1998.
[16] S. Agatzini-Leonardou, P. Oustadakis, P.E. Tsakiridis, C.h. Markopoulos, Titanium leaching from red mud by diluted sulfuric acid at atmospheric pressure, J. Hazard. Mater. 157 (2-3) (2008) 579–586.
[17] E. Erçag, R. Apak, Furnace smelting and extractive metallurgy of red mud: recovery of TiO_2, Al_2O_3 and pig iron, J. Chem. Technol. Biot. 70 (3) (1997) 241–246.
[18] T.K. Mukherjee, S.P. Chakraborty, A.C. Bidaye, C.K. Gupta, Recovery of pure vanadium oxide from bayer sludge, Miner. Eng. 3 (3-4) (1990) 345–353.
[19] M. Samouhos, M. Taxiarchou, P.E. Tsakiridis, K. Potirindis, Greek "red mud" residue: a study of microwave reductive roasting followed by magnetic separation for a metallic iron recovery process, J. Hazard. Mater. 254-255 (2013) 193–205.
[20] M. Ochsenkühn-Petropulu, T.h. Lyberopulu, G. Parissakis, Direct determination of landthanides, yttrium and scandium in bauxites and red mud from alumina production, Anal. Chim. Acta 296 (3) (1994) 305–313.
[21] R.A. Chi, The resource and extraction of scandium, Nonfer. Metals Eng. Res. 2 (1993) 10–22.
[22] J. Xiao, Distribution characteristics of scandium in the red mud of industrial wastes, Geol. 2 (1996) 82–86.
[23] H. Zhou, D. Li, Y. Tian, Y. Chen, Extraction of scandium from red mud by modified activated carbon and kinetics study, Rare Met. 27 (3) (2008) 223–227.
[24] P.E. Tsakiridis, S. Agatzini-Leonardou, P. Oustadakis, Red mud addition in the raw meal for the production of Portland cement clinker, J. Hazard. Mater. 116 (1-2) (2004) 103–110.
[25] I. Vangelatos, G.N. Angelopoulos, D. Boufounos, Utilization of ferroalumina as raw material in the production of Ordinary Portland Cement, J. Hazard. Mater. 168 (1) (2009) 473–478.
[26] J.N. Gordon, W.R. Pinnock, M.M. Moore, A preliminary investigation of strength development in Jamaican red mud composites, Cement Concrete Comp. 18 (1996) 371–379.
[27] B. Singh, G. Ishwarya, M. Gupta, S.K. Bhattacharyya, Geopolymer concrete: a review of some recent developments, Constr. Build. Mater. 85 (2015) 78–90.
[28] N. Zhang, H.H. Sun, X.M. Liu, J.X. Zhang, Early-age characteristics of red mud-coal gangue cementitious material, J. Hazard. Mater. 167 (2009) 927–932.
[29] J. Davidovits, Geopolymer Chemistry and Applications, Geopolymer Institute, 2011.
[30] J.L. Provis, J. Deventer, Alkali Activated Materials: State-of-the-Art Report, RILEM TC 224-AAM, (2014).
[31] P. Duxson, A. Fernandez-Jimenez, J.L. Provis, G.C. Lukey, A. Palomo, J.S.J. van Deventer, Geopolymer technology: the current state of the art, J. Mater. Sci. 42 (2007) 2917–2933.
[32] F. Pacheco-Torgal, J. Castro-Gomes, S. Jalali, Alkali-activated binders: a review. Part 2. About materials and binders manufacture, Constr. Build. Mater. 22 (2008) 1315–1322.
[33] J.L. Provis, S.A. Bernal, Geopolymers and related alkali-activated materials, Annu. Rev. Mater. Res. 44 (2014) 299–327.
[34] J.L. Provis, A. Palomo, C.J. Shi, Advances in understanding alkali-activated materials, Cement Concrete Res. 78 (2015) 110–125.
[35] P. Duxson, J.L. Provis, G.C. Lukey, J.S.J. van Deventer, The role of inorganic polymer technology in the development of 'green concrete', Cement Concrete Res. 37 (2007) 1590–1597.
[36] G. Zhang, J. He, R.P. Gambrell, Synthesis, characterization, and mechanical properties of red mud-based geopolymers, Transport Res. Rec. 2167 (1) (2010) 1–9.
[37] J. He, J. Zhang, Y. Yu, G. Zhang, The strength and microstructure of two geopolymers derived from metakaolin and red mud-fly ash admixture: a comparative study, Constr. Build. Mater. 30 (2012) 80–91.
[38] W. Hajjaji, S. Andrejkovicova, C. Zanelli, M. Alshaaer, M. Dondi, J.A. Labrincha, F. Rocha, Composition and technological properties of geopolymers based on metakaolin and red mud, Mater. Design 52 (2013) 648–654.
[39] Z.H. Pan, D.X. Li, J. Yu, N.R. Yang, Properties and microstructure of the hardened alkali-activated red mud-slag cementitious material, Cement Concrete Res. 33 (2003) 1437–1441.
[40] K. Kaya, S. Soyer-Uzun, Evolution of structural characteristics and compressive strength in red mud-metakaolin based geopolymer systems, Ceram Int. 42 (2016) 7406–7413.
[41] Z.H. Pan, L. Cheng, Y.N. Lu, N.R. Yang, Hydration products of alkali-activated slag-red mud cementitious material, Cem. Concr. Res. 32 (2002) 357–362.
[42] S. Singh, M.U. Aswath, R.V. Ranganath, Effect of mechanical activation of red mud on the strength of geopolymer binder, Constr. Build. Mater. 177 (2018) 91–101.
[43] M. Zhang, T. El-Korchi, G.P. Zhang, J.Y. Liang, M.J. Tao, Synthesis factors affecting mechanical properties, microstructure, and chemical composition of red mud-fly ash based geopolymers, Fuel 134 (2014) 315–325.
[44] J. He, Y.X. Jie, J.H. Zhang, Y.Z. Yu, G.P. Zhang, Synthesis and characterization of red mud and rice husk ash-based geopolymer composites, Cem. Concr. Comp. 37 (2013) 108–118.
[45] X.Y. Ke, S.A. Bernal, N. Ye, J.L. Provis, J.K. Yang, One-part geopolymers based on thermally treated red mud/NaOH blends, J. Am. Ceram. Soc. 98 (2015) 5–11.
[46] B. Guo, D.A. Pan, B. Liu, A.A. Volinsky, M. Fincan, J.F. Du, S.G. Zhang, Immobilization mechanism of Pb in fly ash-based geopolymer, Constr. Build. Mater. 134 (2017) 123–130.
[47] J.G. Zhang, J.L. Provis, D.W. Feng, J.S.J. van Deventer, The role of sulfide in the immobilization of Cr(VI) in fly ash geopolymers, Cement Concrete Res. 38 (2008) 681–688.
[48] B.I. El-Eswed, R.I. Yousef, M. Alshaaer, I. Hamadneh, S.I. Al-Gharabli, F. Khalili, Stabilization/solidification of heavy metals in kaolin/zeolite based geopolymers, Int. J. Miner. Proc. 137 (2015) 34–42.
[49] N. Ye, J.K. Yang, S. Liang, Y. Hu, J.P. Hu, B. Xiao, Q.F. Huang, Synthesis and strength optimization of one-part geopolymer based on red mud, Constr. Build. Mater. 111 (2016) 317–325.
[50] D.S. Kosson, A.C. Garrabrants, R. DeLapp, H.A. van der Sloot, pH-dependent leaching of constituents of potential concern from concrete materials containing coal combustion fly ash, Chemosphere 103 (2014) 140–147.
[51] V. Gella, Precipitation of aluminum (oxy)hydroxides from concentrated chloride solutions by neutralization, 2007.
[52] Z. Sun, A. Vollpracht, H.A. van der Sloot, pH dependent leaching characterization of major and trace elements from fly ash and metakaolin geopolymers, Cement Concrete Res. 125 (2019) 105889.
[53] Z. Sun, A. Vollpracht, Leaching of monolithic geopolymer mortars, Cement Concrete Res. 136 (2020) 106161.
[54] P. Hartwich, A. Vollpracht, Influence of leachate composition on the leaching behaviour of concrete, Cem. Concr. Res. 100 (2017) 423–434.
[55] H.A.v.d. Sloot, D. Hoede, R.P.J.J. Rietra, R. Stenger, T. Lang, M. Schneider, G. Spanka, E. Stoltenberg-Hansson, A. Lerat, Environmental criteria for cement based products ECRICEM Phase I: Ordinary Portland Cements, in, Energy Research Centre of the Netherlands, 2001.
[56] J.J. Dijkstra, H.A.v.d.S. G, Dossier of Information Justifying That Concrete Qualifies for the Potential Release of Regulated Dangerous Substances Without-Further-Testing (WFT) by the Producer, ECN-X-13-008, 2013.
[57] Deutsches Institut für Bautechnik (DIBt), Muster-Verwaltungsvorschrift Technische Baubestimmungen (MVVTB), Appendix 10, in, Berlin, 2017.
[58] A. Vollpracht, W. Brameshuber, Binding and leaching of trace elements in Portland cement pastes, Cement Concrete Res. 79 (2016) 76–92.
[59] CEN/TS 16637-2, Assessment of Release of Dangerous Substances - Part 2: Horizontal Dynamic Surface Leaching Test, 2014.
[60] A. Vollpracht, B. Lothenbach, R. Snellings, J. Haufe, The pore solution of blended cements: a review, Mater. Struct. 49 (8) (2016) 3341–3367.
[61] I. Garcia-Lodeiro, A. Palomo, A. Fernandez-Jimenez, D.E. Macphee, Compatibility studies between N-A-S-H and C-A-S-H gels. Study in the ternary diagram Na_2O-CaO-Al_2O_3-SiO_2-H_2O, Cem. Concr. Res. 41 (2011) 923–931.
[62] J.G. Zhang, J.L. Provis, D.W. Feng, J.S.J. van Deventer, Geopolymers for immobilization of Cr^{6+}, Cd^{2+}, and Pb^{2+}, J. Hazard. Mater. 157 (2008) 587–598.
[63] A. Palomo, M. Palacios, Alkali-activated cementitious materials: alternative matrices for the immobilisation of hazardous wastes – Part II. Stabilisation of chromium and lead, Cem. Concr. Res. 33 (2003) 289–295.
[64] A. Al-Mashqbeh, S. Abuali, B. El-Eswed, F.I. Khalili, Immobilization of toxic inorganic anions ($Cr_2O_7^{2-}$, MnO_4 and $Fe(CN)_6^{3-}$) in metakaolin based geopolymers: a preliminary study, Ceram. Int. 44 (5) (2018) 5613–5620.
[65] B.I. El-Eswed, O.M. Aldagag, F.I. Khalili, Efficiency and mechanism of stabilization/solidification of Pb(II), Cd(II), Cu(II), Th(IV) and U(VI) in metakaolin based geopolymers, Appl. Clay Sci. 140 (2017) 148–156.